Crystal Nucleation, Growth, and Morphology of the Synthetic Malaria Pigment β-Hematin and the Effect Thereon by Quinoline Additives: The Malaria Pig-ment as a Target of Various Ant...

ARTICLE *in* JOURNAL OF THE AMERICAN CHEMICAL SOCIETY · APRIL 2007

Impact Factor: 12.11 · DOI: 10.1021/ja0674183 · Source: PubMed

J|A|C|S
ARTICLES
Published on Web 02/10/2007

Crystal Nucleation, Growth, and Morphology of the Synthetic Malaria Pigment β-Hematin and the Effect Thereon by Quinoline Additives: The Malaria Pigment as a Target of Various Antimalarial Drugs

Inna Solomonov,[†] Maria Osipova,[†] Yishay Feldman,[‡] Carsten Baehtz,[§] Kristian Kjaer,[||] Ian K. Robinson,[⊥] Grant T. Webster,[#] Don McNaughton,[#] Bayden R. Wood,[#] Isabelle Weissbuch,*[,†] and Leslie Leiserowitz*[,†]

Contribution from the Department of Materials and Interfaces, The Weizmann Institute of Science, 76100-Rehovot, Israel, Chemical Research Support, The Weizmann Institute of Science, 76100-Rehovot, Israel, Hasylab at DESY, Notkestrasse 85, D-22607 Hamburg, Germany, Niels Bohr Institute, University of Copenhagen, Universitetsparken 5, DK-2100 Copenhagen, Denmark, Department of Physics and London Centre for Nanotechnology, University College, Gower Street, London WC1E 6BT, England, and Centre for Biospectroscopy and School of Chemistry, Monash University, 3800 Victoria, Australia

Received October 17, 2006; E-mail: isabelle.weissbuch@weizmann.ac.il; leslie.leiserowitz@weizmann.ac.il

Abstract: The morphology of micrometer-sized β-hematin crystals (synthetic malaria pigment) was determined by TEM images and diffraction, and by grazing incidence synchrotron X-ray diffraction at the air−water interface. The needle-like crystals are bounded by sharp {100} and {010} side faces, and capped by {011} and, to a lesser extent, by {001} end faces, in agreement with hemozoin (malaria pigment) crystals. The β-hematin crystals grown in the presence of 10% chloroquine or quinine took appreciably longer to precipitate and tended to be symmetrically tapered toward both ends of the needle, due to stereoselective additive binding to {001} or {011} ledges. Evidence, but marginal, is presented that additives reduce crystal mosaic domain size along the needle axis, based on X-ray powder diffraction data. Coherent grazing exit X-ray diffraction suggests that the mosaic domains are smaller and less structurally stable than in pure crystals. IR-ATR and Raman spectra indicate molecular based differences due to a modification of surface and bulk propionic acid groups, following additive binding and a molecular rearrangement in the environment of the bulk sites poisoned by occluded quinoline. These results provided incentive to examine computationally whether hemozoin may be a target of antimalarial drugs diethylamino-alkoxyxanthones and artemisinin. A variation in activity of the former as a function of the alkoxy chain length is correlated with computed binding energy to {001} and {011} faces of β-hematin. A model is proposed for artemisinin activity involving hemozoin nucleation inhibition via artemisinin−β-hematin adducts bound to the principal crystal faces. Regarding nucleation of hemozoin inside the digestive vacuole of the malaria parasite, nucleation via the vacuole's membranous surface is proposed, based on a reported hemozoin alignment. As a test, a dibehenoyl-phosphatidylcholine monolayer transferred onto OTS−Si wafer nucleated far more β-hematin crystals, albeit randomly oriented, than a reference OTS−Si.

Introduction

Malaria, a tropical disease caused by protozoan parasites of the genus *Plasmodium*, has been a primary concern to humanity for centuries and is now extended to more than 40% of the world's population. *Plasmodium falciparum*, the most prevalent species across the globe, is often fatal to humans. During its life stages within the red blood cell, the malaria parasite degrades host hemoglobin as a major source of amino acids. During this proteolysis in an acidic digestive vacuole, free heme, ferriprotoporphyrin IX (Figure 1a), which is toxic to the parasite, is released. But the heme is converted into a crystalline compound called malaria pigment or hemozoin that is harmless to the parasite.

This crystalline product is isostructural[1] with the synthetic phase β-hematin, the crystal structure of which has been solved from its synchrotron X-ray diffraction powder pattern by Bohle and co-workers.[2] The crystal structure, which had previously been assumed to be built of polymeric chains,[3] was shown to be centrosymmetric, space group $P\bar{1}$, consisting of propionate-

[†] Department of Materials and Interfaces, The Weizmann Institute of Science.
[‡] Chemical Research Support, The Weizmann Institute of Science.
[§] Hasylab at DESY.
[||] Niels Bohr Institute, University of Copenhagen.
[⊥] Department of Physics and London Centre for Nanotechnology, University College.
[#] Centre for Biospectroscopy and School of Chemistry, Monash University.

(1) Oliveira, M. F.; Kycia, S. W.; Gomez, A.; Kosar, A. J.; Bohle, D. S.; Hempelmann, E.; Menezes, D.; Vannier-Santos, M. A.; Oliveira, P. L.; Ferreira, S. T. *FEBS Lett* **2005**, *579*, 6010.

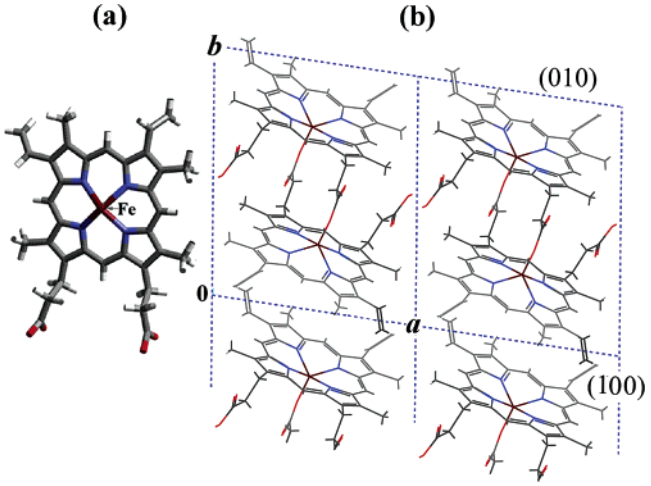

Figure 1. (a) The heme molecular structure. (b) Crystal structure of β-hematin, which consists of molecular heme dimers, viewed along the *c*-axis. The (100) and (010) faces are labeled.

linked (Fe−O−C(=O)CH_2CH_2−) reciprocal head-to-tail cyclic heme dimers interlinked via O−H···O=C hydrogen-bonded cyclic pairs forming chains aligned parallel to the axial direction $a-c$ (Figure 1b). This crystal structure led Bohle et al.[2] to propose, in keeping with previous similar suggestions,[4,5] that antimalarial quinoline-type drugs act by binding to hemozoin crystal faces, which would inhibit their growth and result in a buildup of the toxic heme and thus lead to the death of the parasite. However, no information on the crystal surface binding site was provided, nor details on the habit and $\{h,k,l\}$ faces of the micrometer-sized hemozoin or β-hematin crystals, in terms of the crystal structure.

By making use of the crystal structure of β-hematin, we have reported its theoretical growth morphology[6] (Figure 2a) which has been shown to be similar in habit and form to that of several reported specimens of hemozoin.[7] A model of binding quinoline drugs to the fast-growing highly corrugated {001} face of hemozoin, shown in Figure 2b for binding of chloroquine, was also determined by theoretical methods,[6] but direct experimental evidence of this binding site was still absent.

The mode of action of quinoline-containing drugs and recently developed resistance to commonly used quinolines by malaria parasites has been recently reviewed by Bray et al.[8] Indeed, it is this resistance, made manifest by reduced drug accumulation in the food vacuole that has motivated the need for a fuller understanding of the mode of action of quinoline drugs and the development of new, effective antimalarial drugs.

Here we describe experiments to glean information on the crystal nucleation process of β-hematin. We use as a basis the fact that the β-hematin molecular dimer is a bolaform amphiphile, the observation that β-hematin crystal formation can be enhanced by the presence of lipids,[9] and the report by Goldberg and co-workers[10] of aligned parallelepiped crystals of hemozoin formed in the digestive vacuole of *Plasmodium falciparum*. It is well-established that crystalline monolayers of amphiphilic molecules induce oriented nucleation of molecular crystals at the amphiphilic−aqueous solution interface by virtue of structural complementarity between the head groups of the monolayer and the layer arrangement within the to-be-nucleated crystal. Thus, we examined the nucleation behavior of β-hematin crystals at an air−water interface and at the interface between a phospholipid monolayer on solid support and a chloroform solution. We present here a characterization of the β-hematin crystal morphology obtained from different solvents in relation to its crystal structure, as well as observed changes in the morphology, time of precipitation, and a possible reduction in domain size of crystals grown in the presence of quinine and chloroquine additives. Experimental evidence in favor of the binding of the quinoline to β-hematin at the surface of the growing crystal is also presented. Various experimental techniques, described in the Supporting Information (SI), were applied to obtain the above information, including grazing incidence X-ray diffraction (GIXD), electron diffraction (ED), transmission electron microscopy (TEM) images, synchrotron X-ray powder diffraction (XRPD), coherent grazing exit synchrotron X-ray scattering, micro-Raman spectroscopy, and IR attenuated total reflectance (ATR) micro-imaging spectroscopy. Micro-Raman and IR-ATR spectroscopies have recently been used to understand the electronic structure of β-hematin and hemozoin in whole red blood cells[11] and are shown to be a useful way of monitoring heme aggregation through specific marker bands in human red blood cells.[12]

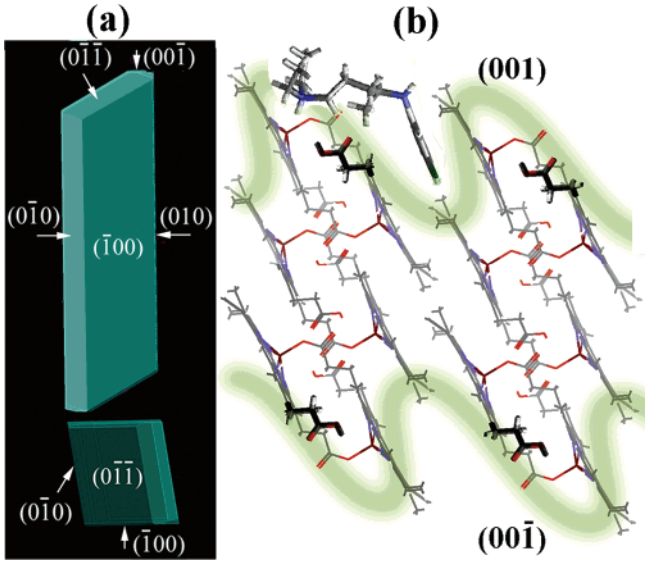

Figure 2. (a) Theoretical growth form of β-hematin viewed: (top) perpendicular to the {100} face, (bottom) along the *c*-axis; (b) corrugated {001} faces of β-hematin, at which adsorption of quinoline drugs has been proposed, as shown for chloroquine bound to the (001) face.[6]

(2) Pagola, S.; Stephens, W. P.; Bohle, D. S.; Kosar, A. D.; Madsen, S. K. *Nature* **2000**, *404*, 307.
(3) Slater, A. F. G.; Swiggart, W. J.; Orton, B. R.; Flitter, W. D.; Goldberg, D. E.; Cerami, A.; Henderson, G. B. *Proc. Natl. Acad. Sci. U.S.A.* **1991**, *88*, 325.
(4) Sullivan, D. J.; Gluzman, I. Y.; Russell, D. G.; Goldberg, D. E. *Natl. Acad. Sci. U.S.A.* **1996**, *93*, 11865.
(5) Sullivan, D. J.; Matile, H.; Ridley, R. G.; Goldberg, D. E. *J. Biol. Chem.* **1998**, *273*, 31103.
(6) Buller, R.; Peterson, M. L.; Almarsson, O.; Leiserowitz, L. *Cryst. Growth Des.* **2002**, *2*, 553−562.
(7) Chen, M. M.; Shi, L.; Sullivan, D. J. *Mol. Biochem. Parasitol.* **2001**, *113*, 1.
(8) Bray, P. G.; Ward, S. A.; O'Neill, P. M. *Drugs, Disease and Post-genomic Biology, Current Topics in Microbiology and Immunology*; Springer-Verlag: Berlin, Heidelberg, 2005; Vol. 295.
(9) Fitch, C. D.; Cai, G. Z.; Shen, Y. F.; Shoemaker, J. D. *Biochim. Biophys. Acta* **1999**, *1454*, 31.
(10) Goldberg, D. E.; Slater, A. F. G.; Cerami, A.; Henderson, G. B. *Proc. Natl. Acad. Sci. U.S.A.* **1990**, *87*, 2931−2935.
(11) Wood, B. R.; Langford, S. J.; Cooke, B. M.; Lim, J.; Glenister, F. K.; Duriska, M.; Unthank, J. K.; McNaughton, D. *J. Am.. Chem. Soc.* **2004**, *126*, 9233−9239.

Chart 1. Generalized Structure of 3,6-Bis-ω-*N*,*N*-diethylamino-alkoxyxanthones, Labeled XN*n*, where *n* is the Number of CH_2 Groups

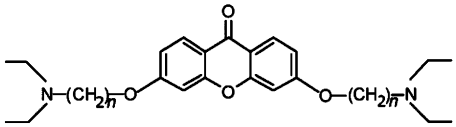

Next we examine by computational means the possibility of hemozoin nucleation/growth inhibition as an important factor in the antimalarial activity of drugs other than quinolines, focusing on diethylamino-alkoxyxanthones and artemisinin. The binding properties of 3,6-bis-ω-diethylamino-alkoxyxanthones (Chart 1) to the surface crystal structure of β-hematin are examined in terms of the antimalarial activity of the drug, which belongs to a novel class of antimalarial compounds with activity against multidrug-resistant *Plasmodium* parasites, reported by Riscoe and co-workers.[13,14]

These compounds, labeled XN*n*, where *n* is the number of CH_2 groups per chain ranging from 2 to 8 (except $n = 7$), form soluble complexes with heme and prevent the precipitation of heme in aqueous solution under the mildly acidic conditions of the parasitic digestive vacuole at pH = 5.2. A strong correlation was found between the heme affinity (K_a) measured in aqueous solution, the alkoxy chain length, and antimalarial potency,[13] shown in Figure S1of the SI. The two most active compounds in the series, $n = 5$ and 6, exhibited low nanomolar 50% inhibitory concentration (IC_{50}) values against strains of chloroquine-susceptible and multidrug-resistant *Plasmodium falciparum* in vitro.

Finally, we consider inhibition of crystal nucleation/growth of hemozoin as a possible mode of action to account for the widely used antimalarial drug, artemisinin, extracted from an ancient Chinese herbal remedy, *Artemisia annu* (sweet wormwood or "qinghao"). Artemisinin and its derivatives (Chart 2a), being highly active against multidrug-resistant strains of malaria parasite, have attracted much attention; the mechanisms of action, resistance, and toxicity have been recently reviewed by Meshnick[15] and by Bray et al.[8] The reactivity of the peroxide function of artemisinin has been considered as the primary factor of the pharmacological activity. A key finding is that artemisinin cannot be cyclically oxidized and reduced; only one free radical can result from one drug molecule, which has a selective toxic effect at very low concentrations. The selective toxicity of artemisinin may arise from alkylation of the heme leading to heme−artemisinin-derived covalent adducts. Heme−artemisinin adducts have been demonstrated in parasite cultures treated with therapeutic concentrations of artemisinin derivatives.[16] Artemisinin forms covalent bonds with heme when incubated in a cell-free solution, and these same artemisinin−heme adducts appear to form in artemisinin-treated parasites. At micromolar concentrations, artemisinin inhibits hemoglobin digestion by malaria parasites and inhibits hemozoin formation, but this has only been demonstrated in cell-free conditions.[17] The structure

Chart 2. (a) Molecular Structure of Artemisinin, and Two Derivatives; (b) alkylation of Iron(II)−Heme by Artemisinin; in these Heme−Artemisinin Adducts the Substitution May Occur at α, β (as shown), γ, or δ Positions, Yielding Products Aα**H**, Aβ**H**, Aγ**H**, and Aδ**H**, Respectively, where A Represents an Artemisinin Moiety Covalently Bound to a Heme H via Sites α, β, γ, δ

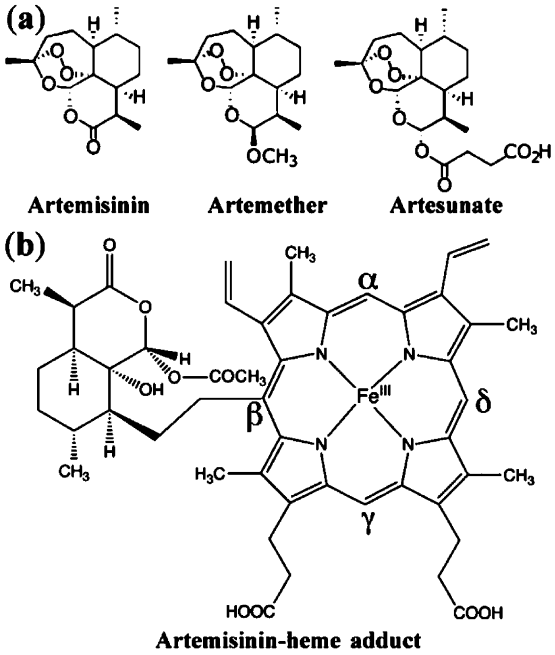

of an artemisinin−porphyrin adduct has been characterized by Meunier and co-workers,[18] following activation of the peroxide function of artemisinin by iron(II)−heme generated in situ from iron(III)−protoporphyrin-IX and glutathione, a biologically relevant reductant. It was found that under mild conditions, such a reaction produced a high yield (85%) of heme derivatives alkylated at α, β, γ, and δ positions by a C4-centered radical derived from artemisinin (Chart 2b), where the regioselectivity at the α, β and δ positions were about the same at 28% on average. The relatively low yield of 13% at the γ-position is presumably due to molecular overcrowding. We shall make use of this structural information to develop a scenario involving hemozoin nucleation inhibition to account for the antimalarial behavior of artemisinin and, as an extension, rationalize the increased antimalarial efficacy when a cocktail of artemisinin and quinoline-type drugs are used in conjunction. We stress, however, that there are various hypotheses on the mechanism of artemisinin-based drug action; besides heme alkylation, a number of other biological targets have been proposed including specific parasite proteins.[8,15]

Results

β-Hematin Crystals at the Air−Water Interface. Little is known on the crystal nucleation of the malaria pigment hemozoin in the digestive vacuole of the malaria parasite. In order to glean some knowledge on the process, albeit indirect, we tried to monitor, by grazing incidence X-ray diffraction (GIXD) using synchrotron radiation, the crystal nucleation of β-hematin (i.e., synthetic hemozoin) in a manner akin to the

(12) Wood, B. R.; Hammer, L.; Davis, L.; McNaughton, D. *J. Biomed. Opt.* **2005**, *10*, 014005/1−01400.5/13.
(13) Kelly, J. X.; Winters, R.; Peyton, D. H.; Hinrichs, D. H.; Riscoe, M. *Antimicrob. Agents Chemother.* **2002**, *46*, 144−150.
(14) Riscoe, M.; Kelly, J. X.; Winter, R. *Curr. Med. Chem.* **2005**, *12*, 2539.
(15) Meshnick, S. H. *Int. J. Parasitol.* **2002**, *32*, 1655−1660.
(16) Hong, Y. L.; Yang, Y. Z.; Meshnick, S. R. *Mol. Biochem. Parasitol.* **1994**, *63*, 121−128.
(17) Pandey, A. V.; Tekwani, B. L.; Singh, R. L.; Chauhan, V. S. *J. Biol. Chem.* **1999**, *274*, 19383.
(18) Robert, A.; Coppel, Y.; Meunier, B. *Chem. Comm.* **2002**, 414−415.

way adopted in following the crystal nucleation of the amphiphile cholesterol from one to three bilayers at the air−water interface.[19] The idea was to take advantage of the fact that the molecular dimeric structure of β-hematin (Figure 1b), the basic building block of the crystal, may be regarded as a bolaform amphiphile and so might form crystalline multilayers at the air−water interface.[20]

When a fresh solution, which contained hemin (chloro(protoporphyrinato)iron(III)) and 2,6-lutidine in chloroform (see experimental details in SI), was spread on water, formation of β-hematin crystals was not detected on examination of the film at the liquid surface by GIXD even after 24 h, nor by FTIR after transfer to solid support. The result remained unchanged when the phospholipid dipalmitoylphosphatidyl-choline or -ethanolamine (DPPC or DPPE), sufficient for about 15% of a full monolayer coverage, was added to the chloroform solution. By contrast, the bulk solutions, yielded β-hematin nanocrystals only after overnight aging, as determined by FTIR and powder X-ray diffraction measurements. For the nanocrystal characterization, samples were prepared by spreading the aged solution on the water surface of a Langmuir trough followed by transferring the insoluble floating material onto a gold-covered silicon wafer. The FTIR spectra obtained were very similar to those of published data,[21] which showed the characteristic strong and narrow bands at 1206 and 1660 cm^{-1}, indicative of the iron-coordinated C−O and C═O stretching vibrations which are absent in hemin. The X-ray powder diffraction pattern matched that of published data.[2] An aged bulk solution, when spread on the water surface, yielded β-hematin crystals floating mainly on their {100} face, according to GIXD and X-ray reflectivity measurements[20,22−24] of the film measured on water (Figure 3) performed on the liquid surface diffractometer at Hasylab. Along the a^*-direction, namely perpendicular to the plane of the {100} face, the domain size of these floating crystals was found to be in the range between 200 and 450 Å, determined from the widths of several {100} Bragg peaks by application of the Scherrer formula.[25] The {100} Bragg reflection of one sample preparation is shown in Figure 3b.

Induced Nucleation of β-Hematin Crystals by a Dibehenoyl-L-α-phosphatidylcholine (DBPC) Monolayer. A well-compressed monolayer of DBPC on the water surface of a Langmuir trough was transferred by the Langmuir−Schaffer technique onto an OTS−Si wafer (see experimental details in SI). The DBPC−OTS−Si wafer was oriented vertically, together with an OTS−Si wafer used as reference, in a vessel containing a chloroform solution of hemin and 2,6-lutidine. The number of β-hematin crystals formed on the DBPC−OTS−Si wafer was much greater than on the OTS−Si wafer, according to visual inspection. An initial measure of the orientation of the β-hematin crystals was determined by a specular X-ray diffraction $\theta/2\theta$ scan (see SI), sensing only crystallographic planes parallel to the plane of a Si wafer, as shown in Figure 4.

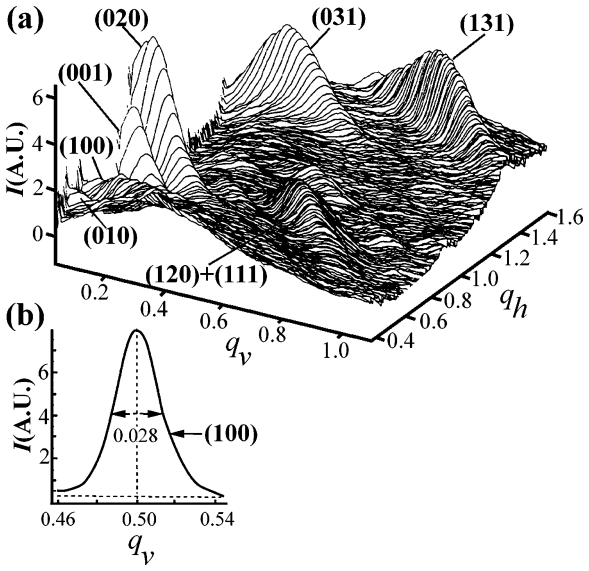

Figure 3. Oriented β-hematin crystallites on the water surface. (a) The GIXD pattern $I(q_h, q_v)$, in which the X-ray scattering vector components q_h and q_v (in $Å^{-1}$) are parallel (i.e., *horizontal*) and perpendicular (i.e., *vertical*) to the water surface respectively. The q_h and q_v values of the various (h,k,l) reflections correspond to β-hematin crystals floating on their *bc* face. This assignment is in agreement with the {100} reflection of β-hematin crystallites obtained from X-ray reflectivity (XR, $q_h \equiv 0$ $Å^{-1}$) measurements depicted in (b). The FWHM of the XR peak (0.028 $Å^{-1}$) corresponds to crystal coherence length L along the direction a^* of 200 Å, applying the Scherrer formula $L = 0.9 \times 2\pi/\text{FWHM}$.[25] Note that the observation of a (100) reflection, albeit very weak, near the horizon ($q_v \approx 0$ $Å^{-1}$) in the GIXD pattern (a) indicates that there is a very small population of crystals floating on their *ac* faces.

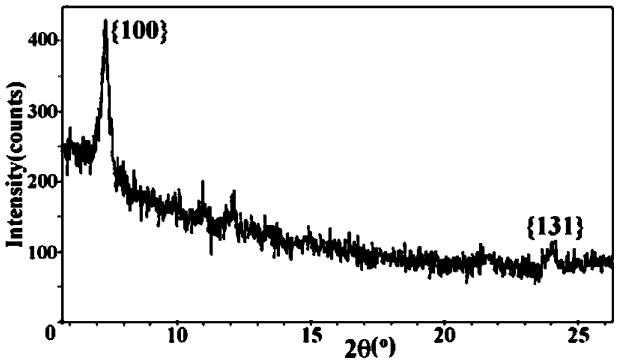

Figure 4. Specular X-ray (wavelength $\lambda = 1.542$ Å) diffraction $\theta/2\theta$ scan probing the orientation of β-hematin crystals nucleated by the exposed polar head groups of a phospholipid DBPC monolayer in contact with an OTS−Si wafer. The {100} and {131} reflections are denoted.

The intense {100} reflection suggests some measure of preferred orientation when comparing the intensities of the {100} and {131} reflections with those of the corresponding reflections in Figure 8c (vide infra), but a pole figure of the {100} reflection showed only a very minor preference for the {100} faces to lie parallel to the surface plane of the DBPC−OTS−Si wafer, the overriding majority of crystals were randomly oriented.

Morphology of Pure β-Hematin Crystals. According to the theoretical growth morphology of β-hematin crystals,[6] in keeping with images of several specimen hemozoin crystals reported by Sullivan and co-workers,[7] the crystals, elongated

(19) Solomonov, I.; Weygand, M. J.; Kjaer, K.; Rapaport, H.; Leiserowitz, L. *Biophys. J.* **2005**, *88*, 1809.
(20) Kuzmenko, I.; Rapaport, H.; Kjaer, K.; Als-Nielsen, J.; Weissbuch, I.; Lahav, M.; Leiserowitz, L. *Chem. Rev.* **2001**, *101*, 1659−1696.
(21) Egan, T. J.; Mavuso, M. W.; Ncokazi, K. K. *Biochemistry* **2000**, *40*, 204−213.
(22) Als-Nielsen, J.; Kjaer, K. In *Proceedings of the Nato Advanced Study Institute, Phase Transitions in Soft Condensed Matter*; Riste, T., Sherrington, D., Eds.; Plenum Press: New York: Geilo, Norway, 1989; Vol. 211, Series B, pp 113−138.
(23) Kjaer, K. *Physica* **1994**, *198*, 100.
(24) Als-Nielsen, J.; Jacquemain, D.; Kjaer, K.; Leveiller, F.; Lahav, M.; Leiserowitz, L. *Phys. Rep.* **1994**, *246*, 251−313.
(25) Guinier, A. *X-ray Diffraction*; Freeman: San Francisco, 1968.

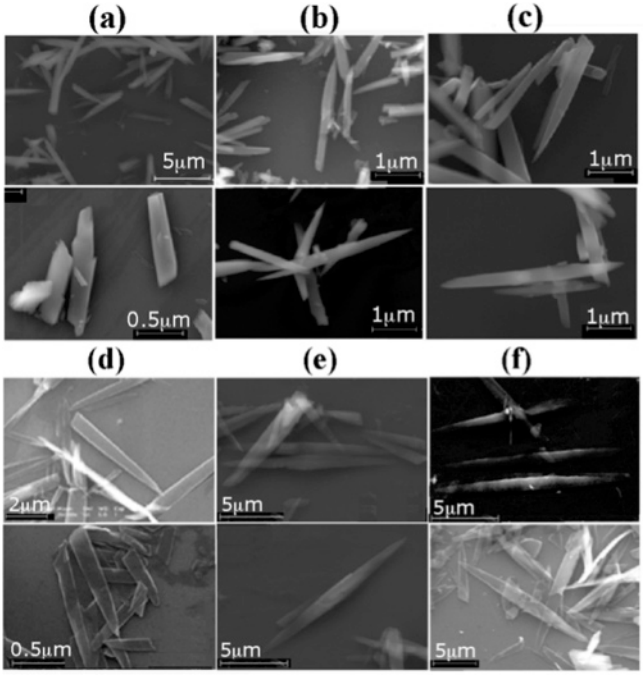

Figure 5. SEM micrographs of β-hematin crystals obtained from: (a−c) MeOH−DMSO and (d−f) $CHCl_3$ solutions. The crystals grown in the absence of the quinolines are shown in (a) and (d); those grown in the presence of 10% quinine and chloroquine are shown in (b, e) and (c, f), respectively.

in the *c*-direction, are delineated by well-developed {100} and {010} side faces and smaller {011} end faces (Figure 2a). In order to experimentally establish this morphology, use was made of TEM images and ED patterns. Here advantage was taken of the small angles between the real (*a*,*b*,*c*) and reciprocal (*a**,*b**,*c**) crystal axes (10°, 8°, 7° respectively) of β-hematin[26] in order to obtain {0*kl*} or {*h*0*l*} diffraction patterns assuming that the crystals would lie on their {100} or {010} faces respectively.

The β-hematin crystals, (grown in MeOH−DMSO[27] or chloroform, see SI), examined by scanning electron microscopy (SEM), appear lath-like in shape, 0.5−10 μm long and 0.05−0.5 μm wide (Figure 5a, d). Several crystals exhibit regular morphologies in keeping with the centrosymmetric $P\bar{1}$ symmetry of the crystal structure. Other crystals tend to be wedge-shaped at one end. We have identified the crystal faces making use of the more regular shaped habit. ED patterns of β-hematin crystals grown in MeOH−DMSO solutions are of the type 0*kl* and *h*0*l* (Figure 6a, b bottom); the corresponding transmission electron microscopy (TEM) images are shown in Figure 6a, b, top. Given the small angles between the real (*a*,*b*,*c*) and corresponding reciprocal (*a**,*b**,*c**) crystal axes (vide supra), the β-hematin crystals displayed in Figure 6a, b lie on their {100} and {010} faces respectively. Of 13 crystals from MeOH−DMSO solution, characterized by TEM micrographs, 11 exposed {010} faces, the remaining two {100} faces. Thus, we may conclude that β-hematin crystals obtained from MeOH−DMSO solutions are tabular needles extended along the *c*-axis, with {010} and {100} side faces, the former being generally more well-developed. A measure of the relative sizes of the exposed {010} and the {100} side faces of a specimen crystal was obtained from a comparison of TEM images of the crystal in its flat position and rotated about its needle axis by 45° (not shown), yielding a width-to-thickness ratio of about 3:1, which is consistent with the observation that most of the crystals observed lay on their {010} face.

The crystals grown in $CHCl_3$ solution expose the {100} face in five of the seven TEM images examined, the remainder the {010} face. The TEM image of a {100} oriented crystal and its corresponding ED pattern are shown in Figure 6c. Thus, the plate and side faces are primarily of the type {100} and {010} respectively for crystals grown in $CHCl_3$ solution.

According to the measurements of several well-formed specimen crystals, four of which are shown in Figure 6a, the edge of the slanted end face makes an angle of 116 ± 4° with the long *c*-axis of the crystal, consistent with an end face of the type {011}, which is the stable end face of the theoretical growth form of β-hematin, and which also appears in several hemozoin specimen crystals.[6] This assignment is consistent with the corresponding ED pattern (Figure 6a, bottom) showing that the diffraction vector *d**(011) is perpendicular to the slanted end face. It is noteworthy that the 0*kl* reciprocal lattice of β-hematin has near *mm* symmetry, the angle between the axes *b** and *c** being 88.8°. Thus, the vectors *d**(011) and *d**(0$\bar{1}$1) are nearly related by mirror symmetry (Figure 6a, bottom) and so it would be difficult to differentiate between slanted faces {011} and {0$\bar{1}$1} by visual inspection only of the TEM image of a specimen crystal. On theoretical grounds, we may preclude formation of the {0$\bar{1}$1} face as commonly occurring, its crystal surface structure being highly corrugated (not shown) and therefore much less stable than the {011} crystal face in accordance with the theoretical crystal growth form computations.[6]

Nucleation and Morphology of β-Hematin Crystals Grown in the Presence of Quinolines. According to our recent study,[6] quinoline-type drugs should inhibit nucleation and growth of hemozoin crystals along the fast-growing *c*-direction as a result of proposed binding onto the {001} faces (Figure 2b), but direct experimental evidence for this model was still missing. In order to provide information on quinoline binding, we examined to what extent the quinoline drugs affected β-hematin crystal nucleation and growth, in terms of time of crystal appearance and change in morphology. Regarding the first question, we found that the presence of 10% quinoline-type additives in chloroform solutions of hemin significantly increased the time for the crystals to appear, indicating a strong inhibition at the nucleation stage. For example, under the experimental conditions used, "pure" β-hematin nanocrystals appeared from chloroform solution after aging for about 12 h (on the basis of 40 experiments). When 10% quinine (Q) or chloroquine (CQ) (mol/mol hemin) was present in the solution, the "drug-affected" crystals appeared with high reproducibility after at least 48 h aging. The time was established from the data of 40 experiments for each additive. Increasing the additive concentration to 20% prevented formation of β-hematin crystals. These data support the comprehensive studies by Egan and co-workers[28] and by

(26) Real and reciprocal unit cell dimensions (Å, Å^{-1}, deg) of β-hematin: a = 12.196 Å, b = 14.684 Å, c = 8.040 Å, α = 90.22, β = 96.80, γ = 97.92, a^* = 0.08338, b^* = 0.06876, c^* = 0.12527, α^* = 88.83° β^* = 83.05°, γ^* = 82.00°. Angles between axes a and a^*, b and b^*, and c and c^*, are 10.5°, 7.9° and 6.8°, respectively.

(27) Bohle, D. S.; Kosar, A. D.; Stephens, W. P. *Acta Crystallogr.* **2002**, *D58*, 1752−1756.

(28) Egan, T. J.; Ross, D. C.; Adams, P. A. *FEBS Lett.* **1994**, *352*, 54−57.

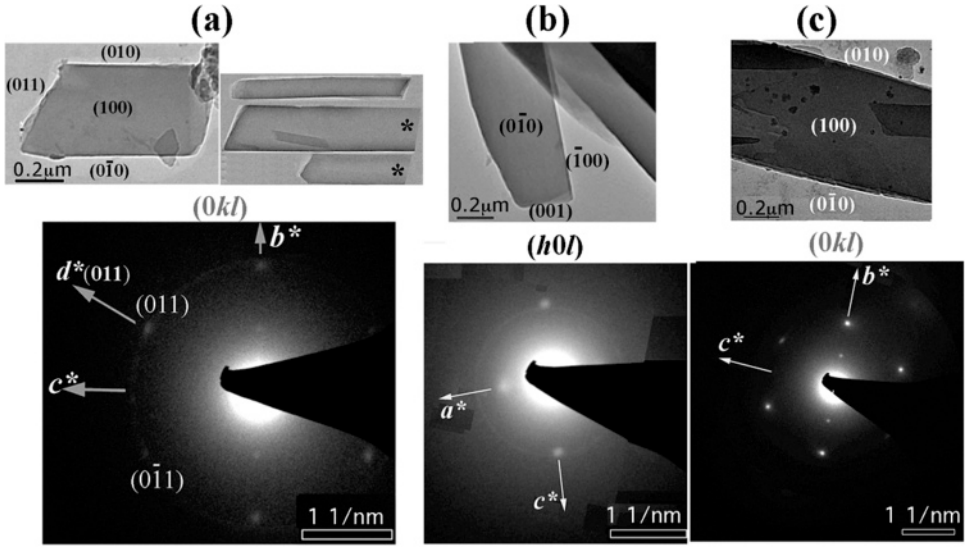

Figure 6. TEM images (top) and corresponding selected-area ED patterns (bottom) of β-hematin crystals obtained from: (a, b) MeOH−DMSO and (c) $CHCl_3$ solutions. The crystal faces are (h,k,l) indexed, based on the corresponding ED pattern. The 0kl diffraction pattern shown in (a) is from the labeled crystal. The morphologies of three other similarly shaped crystals are shown. The ends of the two crystals denoted by an asterisk were cut off from view in the original TEM image.

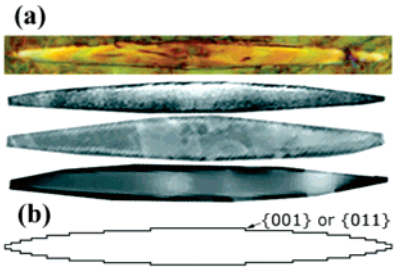

Figure 7. (a) Symmetrically tapered crystals of β-hematin obtained from growth in the presence of the quinoline drugs. The colored crystal was photographed on an optical microscope; the others are from TEM images. (b) Model of stepped face morphology showing {001} and {011} ledges to account for the symmetric tapering.

Chong and Sullivan,[29] which demonstrated that quinoline antimalarials decrease the rate of β-hematin formation.

As for providing evidence that the quinoline-type drugs modify the morphology of the synthetic hemozoin crystals, many of the crystals grown in the presence of CQ and Q were symmetrically tapered at both ends, spine-like in habit (Figure 5b, c, e, f and Figure 7a), primarily those obtained from $CHCl_3$ solution. The average angle between the tapered side faces of four of such spines, shown in Figure 7a is about 11°, in keeping with formation of a stepped-face morphology composed of a series of narrow {001} or {011} facet-type ledges, with an average height/width ratio of $tan5.5° \approx 10$, shown schematically in Figure 7b. We propose that such tapering, resulting in growth along the spine axis of thinner and thinner cross-section, reduces the inhibiting effect of the quinoline additive since adsorption occurs primarily on the exposed {011} or {001} ledges.

Detection of the Effect of Quinolines via X-ray Diffraction Methods and Vibrational Micro-Raman and IR-ATR Spectroscopy. In order to glean more direct evidence of crystal growth inhibition at the {001} or {011} faces by stereoselective adsorption thereon of quinoline additives, we applied the concept that the additive, if adsorbed and perhaps occluded via particular crystal faces, should induce a reduction of the crystal mosaic domain size along the corresponding directions. Thus, use was made of synchrotron X-ray powder diffraction (XRPD) and coherent grazing X-ray diffraction[30] (CGXD) in order to detect such an affect, if present.

A quinoline additive, if adsorbed and occluded via a particular {hkl} face, should result in a reduction of the crystal coherence length L{h,k,l} along the direction perpendicular to that face, as would be made manifest by a broadening of the {hkl} Bragg reflection. L{h,k,l} may be derived from the FWHM of the Bragg reflection by use of the Scherrer formula.[25] Such a concept had been demonstrated by a comparison of the crystal mosaic domain sizes of pure synthetic and biogenic calcite.[31] Thus, quinoline, if adsorbed and occluded via the {001} or {011} face in sufficient concentration, should reduce the crystalline mosaic domain size along the c-direction, resulting in broader {001} or {011} X-ray reflections than those of the pure samples. Thus, synchrotron XRPD measurements[32] (see SI) were performed at Hasylab (Hamburg) on samples of β-hematin grown from MeOH−DMSO and from $CHCl_3$ solutions, in the absence and in the presence of 10% quinoline additive (Q, CQ). Four of these XRPD patterns are shown in Figure 8.

For the analysis of the results, we have assumed that the crystal coherence along the c-axis L{001} relative to the coherence lengths along the different crystallographic directions L{hkl}, is a measure of the relative change in L{001}. In Table 1 the ratios L{001}/L{hkl}, labeled $L_{001/hkl}$, of five well-resolved and sufficiently intense reflections of each powder sample of the "pure" and "affected" crystals are listed, together with the average values of $L_{001/hkl}$. Growth inhibition along the c-axis should yield a decrease in the average value of $L_{001/hkl}$, which is not apparent for crystals grown in MeOH−DMSO (Table 1a), although there appears to be a marginally positive effect for crystals grown in $CHCl_3$ (Table 1b). We have no knowledge,

(29) Chong, C. R.; Sullivan, D. J. *Biochem. Pharmacol.* **2003**, *66*, 2201−2212.
(30) Pfeiffer, F.; Zhang, W.; Robinson, I. K. *Appl. Phys. Lett.* **2004**, *84*, 1847.
(31) Berman, A.; Hanson, J.; Leiserowitz, L.; Koetzle, T. F.; Weiner, S.; Addadi, L. *Science* **1993**, *259*, 776−779.
(32) Knapp, M.; Baehtz, C.; Ehrenberg, H.; Fuess, H. *J. Synchrotron Radiat.* **2004**, *11*, 328−334.

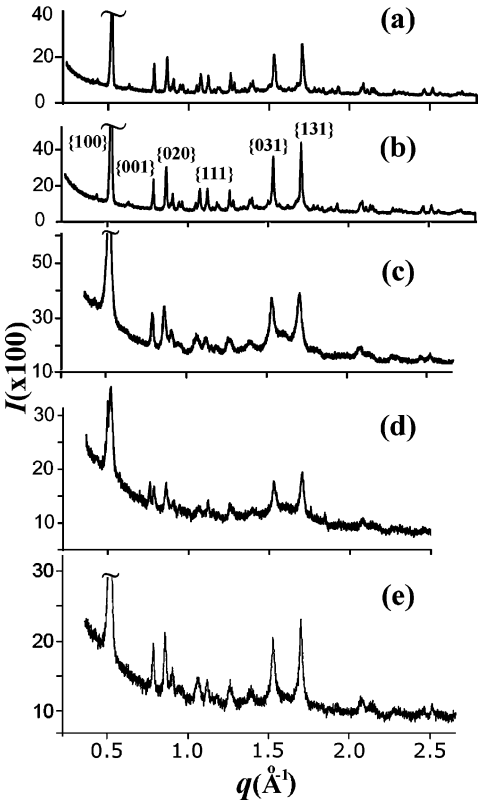

Figure 8. X-ray powder diffraction (XRPD) patterns of β-hematin crystals obtained from (a, b) MeOH−DMSO solution, (c−e) chloroform solution. The XRPD patterns shown in (a, c) correspond to crystals grown in the absence of quinoline additive, those in (b, d, e) to crystals grown in the presence of 10% CQ, Q, and CQ respectively.

Table 1. Crystal Coherence Lengths $L\{hkl\}$ (Å) along Six *hkl* Directions, the Ratios $L\{001\}/L\{hkl\}$, Denoted as $L_{001/hkl}$ and the Average Ratio thereof $\langle L_{001/hkl}\rangle$ along Five *hkl* Directions {100}−{131} Obtained from Different Sets of XRPD Data of β-Hematin, Grown in the Absence of Quinoline Additives (Pure Crystals) and in the Presence of 10% Q and of 10% CQ

pure β-hematin			+10% quinine		+10% chloroquine	
{*hkl*}	$L\{hkl\}$	$L_{001/hkl}$	$L\{hkl\}$	$L_{001/hkl}$	$L\{hkl\}$	$L_{001/hkl}$
Nine Samples of Crystalline Powder obtained from DMSO-MeOH[a]						
{001}	990		1205		1040	
{100}	810	1.22	830	1.45	790	1.31
{020}	550	1.80	670	1.80	610	1.70
{111}	540	1.83	765	1.58	700	1.47
{031}	455	2.18	490	2.46	515	2.02
{131}	500	1.98	505	2.39	510	2.05
		⟨1.80⟩		⟨1.94⟩		⟨1.71⟩
Three Samples of Crystalline Powder Obtained from $CHCl_3$ Solution						
{001}	390		400		470	
{100}	190	2.05	195	2.05	240	1.96
{020}	315	1.24	370	1.08	395	1.19
{111}	245	1.59	415	0.96	295	1.59
{031}	215	1.81	245	1.63	250	1.88
{131}	180	2.17	310	1.29	275	1.71
		⟨1.77⟩		⟨1.40⟩		⟨1.67⟩

[a] Values in each column are the average of three powder samples.

however, of the concentration of quinoline additive stereoselectively adsorbed onto the crystal surface and the fraction thereof eventually occluded into the crystal.

The CGXD experiment produced the diffraction pattern shown in Figure 9 from the crystals grown from MeOH−DMSO solution without additives. The intensity distribution, which is nominally given by the Fourier transform of the shape of the crystal grain, i.e., mosaic domain, that is illuminated, cannot be interpreted simply, but some general conclusions can be drawn. A strain-free perfect crystal should give a locally centrosymmetric diffraction pattern; the lack of symmetry seen here indicates that the crystal is strained. A plate-like shape for the crystal is suggested by the elongation of the diffraction pattern. The crystals grown from MeOH−DMSO in the presence of quinoline additive gave only very weak diffraction signals that disappeared with X-ray exposure. This suggests that the crystal domains grown in the presence of additives were smaller and less structurally stable.

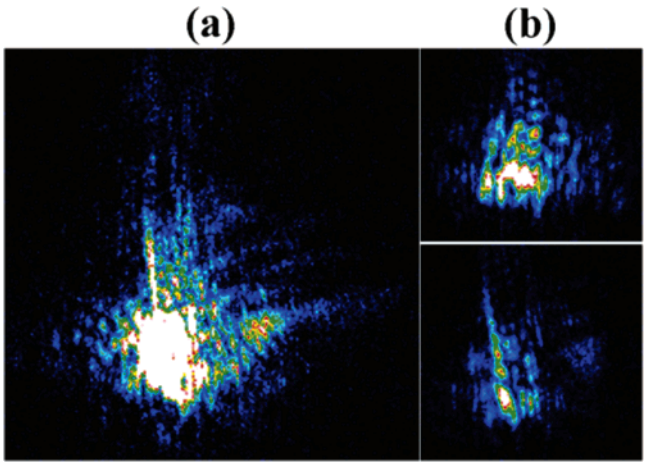

Figure 9. Coherent X-ray diffraction patterns measured for the first peak {100} of the powder diffraction pattern of β-hematin grown without additives: (a) is the center of the rocking curve, whereas in (b) the two smaller panels are offset on either side by a fraction of a degree. The false-color intensity scale is saturated in the center so that the weaker features at the edges of the pattern can be resolved.

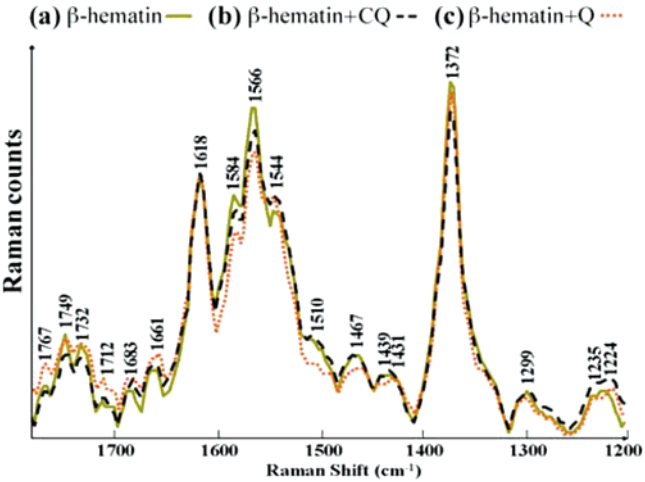

Figure 10. Average micro-Raman spectra in the 1800−1200 cm^{-1} region: (a) pure β-hematin crystals; (b, c) β-hematin grown in the presence of 10% CQ and Q, respectively.

Average micro-Raman spectra[33,34] (see SI) in the 1800−1200 cm^{-1} region of pure β-hematin crystals and β-hematin grown in the presence of 10% quinine and chloroquine (Figure 10) show minor variation, mainly in band widths and relative

(33) Chan, A. K. L.; Kazarian, S. G. *Appl. Spectrosc.* **2003**, *57*, 381−389.
(34) Colley, C. S.; Kazarian, S. G.; Weinberg, P. D.; Lever, M. J. *Biopolymers* **2004**, *74*, 328−335.

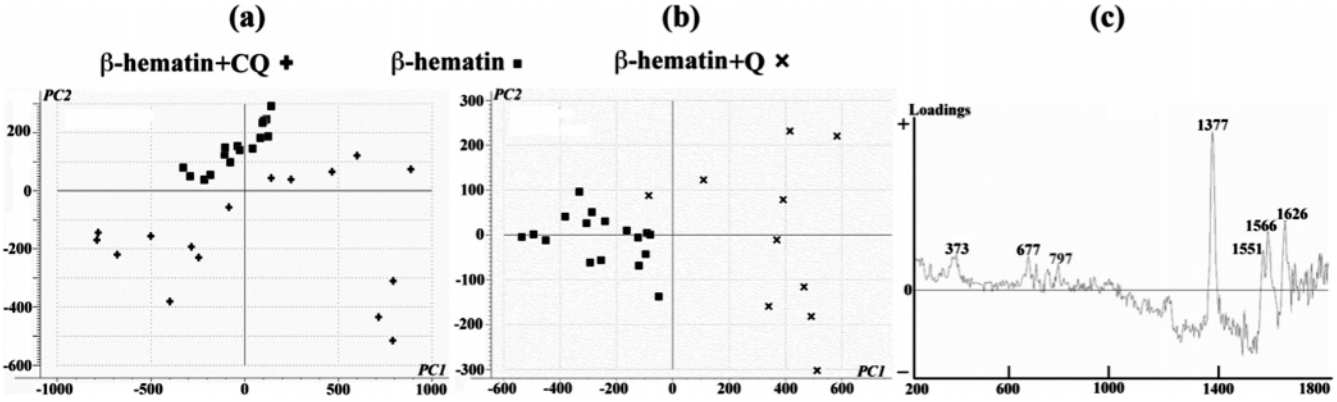

Figure 11. PCA scores plot, PC1 vs PC2 for Raman spectra of (a) pure β-hematin (squares) and β-hematin/chloroquine treated (crosses); (b) pure β-hematin (black squares) and Q-affected β-hematin (crosses); (c) loadings plot for PC1 for (b) with strong positive loadings associated with bands from pure β-hematin and labeled with wavenumber values.

intensity. Band assignments, local symmetry coordinates, symmetry terms, and the spectroscopic notation for β-hematin are based on earlier studies.[11,35]

Bands at 1584 cm^{-1} (assigned to $\nu(C_\alpha C_m)$ of E_u symmetry), 1566 cm^{-1} (assigned to $\nu(C_\beta C_\beta)$ of A_{ig} symmetry also known as ν_2), and 1372 cm^{-1} (assigned to ν(pyrrole half-ring) of A_{1g} symmetry also known as ν_4) appear more intense in the spectra of pure β-hematin crystals compared to those of its drug-affected counterparts. Additionally the band at 1544 cm^{-1} assigned to $\nu(C_\beta C_\beta)$ of B_{1g} (known as ν_{11}) appears less intense in pure β-hematin.

In order to examine variability in the whole dataset of individual spectra principal components analysis (PCA) was used after first preprocessing the data with a multiplicative scatter direction. PCA is a multivariate statistical technique,[36] which breaks the data down into variability within a dataset and allows graphical presentation of the results in the form of scores plots, to determine whether samples group together, and loadings plots, that determine where the variables (in this case spectral wavenumber) that contribute to variance occur. Plots a and b of Figure 11 show PCA scores plots of PC1 vs PC2 for β-hematin grown in the presence of chloroquine (CQ) and quinine (Q), respectively. Each individual score represents a single spectrum plotted as a point in a two-dimensional space, the position of which is dependent on the individual variance contribution of the spectrum to each principal component or basis vector. Overall, pure β-hematin spectra are more tightly clustered than the drug-treated β-hematin spectra in both scores plots, while the quinoline-affected samples have a much larger spectral spread. A distinct separation of the pure β-hematin from that grown in the presence of CQ and Q is observed. For pure β-hematin and CQ-affected β-hematin the separation is mainly along PC2, while for pure β-hematin and Q-affected β-hematin the separation occurs along PC1. Figure 11c depicts the PC1 loadings plot for the β-hematin and Q-affected β-hematin PCA. Bands that have strongly positive or negative loadings are those which are important in explaining the variance and consequently the separation observed in the PC1 vs PC2 scores plot (Figure 11b) between β-hematin and Q-affected β-hematin. The strong positive bands observed in the loadings plot are associated with the pure β-hematin and are mainly of A_{1g} and B_{1g} symmetry and include those at 1626 cm^{-1} (ν_{10}), 1566 cm^{-1} (ν_2), 1551 cm^{-1} (ν_{11}), and 1372 cm^{-1} (ν_4).

The IR-ATR images recorded from β-hematin, CQ-affected β-hematin and Q-affected β-hematin were processed using Cytospec. Each of the three individual images originally contained 4096 spectra in the form of a "spectral hypercube". The spectra were quality tested to remove spectra with low signal/noise and vector normalized, and the second derivative was calculated. Second derivative analysis eliminates the need for baseline correction and sharpens shoulder bands. Band maxima in the raw spectra become minima in the second derivative. The mean second derivative spectrum most representative of the image was determined and extracted using unsupervised hierarchical cluster analysis (UHCA). UHCA is an unsupervised technique used to group similar spectra and is often used for classification in image analysis.[37] Essentially, spectra are clustered by similarity and color coded to form an image. Spectral averages representative of each cluster type can then be extracted. The mean second derivative spectra from the largest cluster (out of a total of four clusters) for each of the conditions are plotted in Figure 12.

The spectra of the CQ-affected β-hematin and Q-affected β-hematin are remarkably similar and distinctly different from pure β-hematin. The band at 1744 cm^{-1} previously attributed to surface propionate groups,[11] but which we now believe to be propionic acid groups, is observed in the spectrum of pure β-hematin but not in the drug-affected samples. There appears to be a shoulder at ~1720 cm^{-1} in the spectra of the drug-affected samples but not in those for pure β-hematin. There are also differences in the bands directly involved in the propionate linkage (to Fe) at ~1660 and 1209 cm^{-1}. A strong shoulder band at ~1670 cm^{-1} can be observed next to the ν(C═O) band at 1657 cm^{-1}, indicating a new carbonyl environment in the drug-affected samples. A close inspection of the C−O band at ~1209 cm^{-1} shows also a slight difference. Distinct differences can also be observed in the 1300−1200 cm^{-1} in drug-affected compared to those of pure β-hematin.

Binding of Diethylamino-alkoxyxanthones (XN*n*) on β-Hematin Crystal Faces and Antimalarial Activity. The relative ability of XN*n* molecules, with $(CH_2)_n$ side chains, $n = 2$ (XN2) and $n = 5$ (XN5), to bind to the crystal surfaces of

(35) Abe, M.; Kitagawa, T.; Kyogoku, K. *J. Chem. Phys.* **1978**, *69*, 4526.
(36) Wood, B. R.; Burden, F. R.; Quinn, M. A.; McNaughton, D. *Biospectroscopy* **1996**, *2*, 145−155.
(37) Wood, B. R.; McNaughton, D. In *Spectrochemical Analyses Using Multichannel Infrared Detectors*; Bhargave, R., Levin, I., Eds.; Blackwell: Cambridge, MA, 2005.

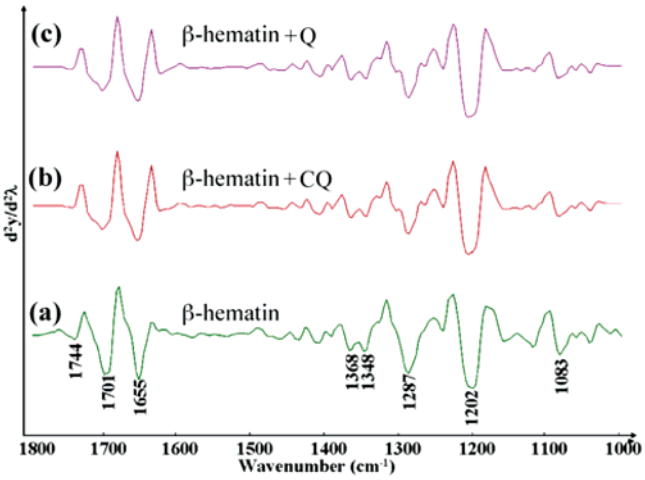

Figure 12. Unsupervised hierarchical cluster analysis (UHCA) cluster average IR spectra (presented as second derivatives) for: (a) β-hematin and (b, c) β-hematin grown in the presence of 10% CQ and Q, respectively. The band at 1744 cm^{-1} in β-hematin, assigned to the carbonyl group of surface propionic acid groups, has disappeared in the drug-treated samples, thus indicating binding through this site.

Table 2. Docking Energies ΔE_b (kcal/mol) of the Diethylamino-hydroxyxanthone Molecules XN2 and XN5 onto the β-Hematin {001} and {011} Crystal Surfaces and the Directions *D* on the Face along Which the Additive Molecules Lie

drug/face	*D*	ΔE_b
	{001}	
XN2	*a*	−25
XN5	*a*	−35
XN5	$2a + b$	−20
	{011}	
XN2	$-b + c$	−5
XN5	*a*	−25

β-hematin was studied by modeling (see SI) the docking of the drug onto the {001} and {011} crystal surfaces. The results are presented in Table 2 and Figure 13.

Artemisinin−Hematin Molecular Dimer Adduct as Inhibitor of Hemozoin Formation. Here we show that the antimalarial drug artemisinin may, in principle, act as a hemozoin growth inhibitor. Meunier and co-workers[18] have demonstrated that artemisinin covalently reacts with the free heme monomer at the three different sites (α, β, δ) on the molecular periphery with about the same regioselectivity of 29%, yielding artemisinin−heme adducts labeled AαH, AβH, and AδH, as depicted in Chart 2b for site β. Reaction at site γ is comparatively low at 13%. We invoke the possibility that each of the four adducts might link to a pure heme monomer in the digestive vacuole of the malaria parasite to form a dimer with a basic skeleton akin to the β-hematin cyclic dimer (Figure 1b), the exact structure thereof depending upon that of the adduct and its relative orientation to the heme monomer prior to dimer formation. Such molecules, if present in the digestive vacuole of the parasite, would act in a manner akin to a classic "tailor-made" additive in solution designed to inhibit crystal nucleation and growth.[38] In principle, four diastereomeric pairs of dimers (labeled AαBH, A$\bar{\alpha}$BH; AβBH, A$\bar{\beta}$BH; AδBH, A$\bar{\delta}$BH; AγBH, A$\bar{\gamma}$BH) may be formed and adsorbed on the six {100}, {010}, and {001} faces of β-hematin.

For the most part, each additive type may be adsorbed at only one of the six faces, as shown somewhat schematically in Figure 14a for binding of the α, $\bar{\alpha}$, β, $\bar{\beta}$, and δ, $\bar{\delta}$ derivatives to the four {100} and {010} crystal side faces. The molecules within each pair are diastereoisomers since artemisinin is chiral and the β-hematin cyclic dimer molecule is centrosymmetric. Using CERIUS[2] software we computed low-energy models of some of the diastereoisomeric dimer structures, which are shown adsorbed onto the different crystal faces in Figure 14b,c.

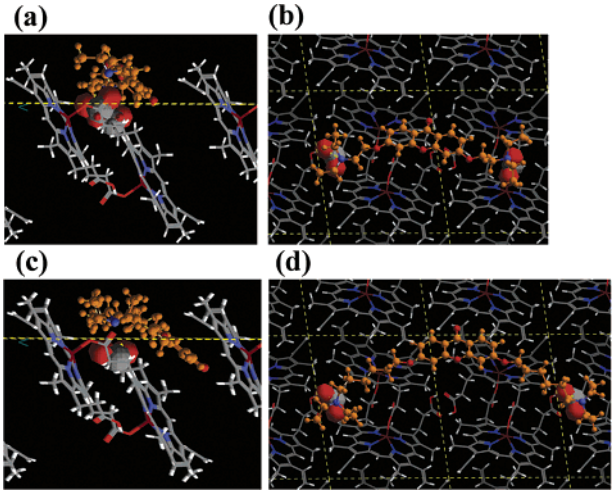

Figure 13. Packing arrangement of β-hematin illustrating the binding to the (001) face of a diethylamino-hydroxyxanthone molecules XN2 shown in (a, b) and XN5 shown in (c, d). Views parallel to the (001) plane (dashed yellow line) are depicted in (a, c) and views perpendicular to the (001) plane are shown in (b, d). The C and H atoms of hydroxyxanthone are colored in orange, the N atoms in blue, and the O atoms in red. The carboxylate O atoms of β-hematin in contact with the NH groups of hydroxyxanthone are large red spheres.

Therefore, on the assumption that the heme−artemisinin reaction products are formed in the digestive vacuole of the parasite in sufficient concentration, an efficient inhibition of growth of hemozoin should occur since the additives may act along all three principal growth directions, *a, b*, and *c*. In principle, only a fraction of the additives can be adsorbed onto the small, but fast-growing {001} faces. Therefore, we may expect a stronger inhibition of crystal growth along this direction to occur were quinoline drugs, such as chloroquine or quinine, used in conjunction with artemisinin, given the proposed mechanism of action of artemisinin. Thus, we examined, via the use of a model crystal system of *S*-alanine as described in the SI, whether a combination of tailor-made crystal nucleation retardants, which inhibit crystal growth along different directions, acts more effectively than each alone. The results suggest that simultaneous use of two types of additives, which bind to different crystal faces, has a greater inhibiting effect on nucleation than each of the additives used alone.

Discussion

Nucleation of Hemozoin Crystals. Little is known at the molecular level on the nucleation process of hemozoin in the digestive vacuole of the parasite, including the critical size of the nucleus, and the role played by various molecules in the vacuole to promote the nucleation process. Attempts to glean information on the critical size of β-hematin nuclei by monitoring the early stages of crystallization of β-hematin at the air−water interface using grazing incidence X-ray diffraction were

(38) Weissbuch, I.; Addadi, L.; Lahav, M.; Leiserowitz, L. *Science* **1991**, *253*, 637−645.

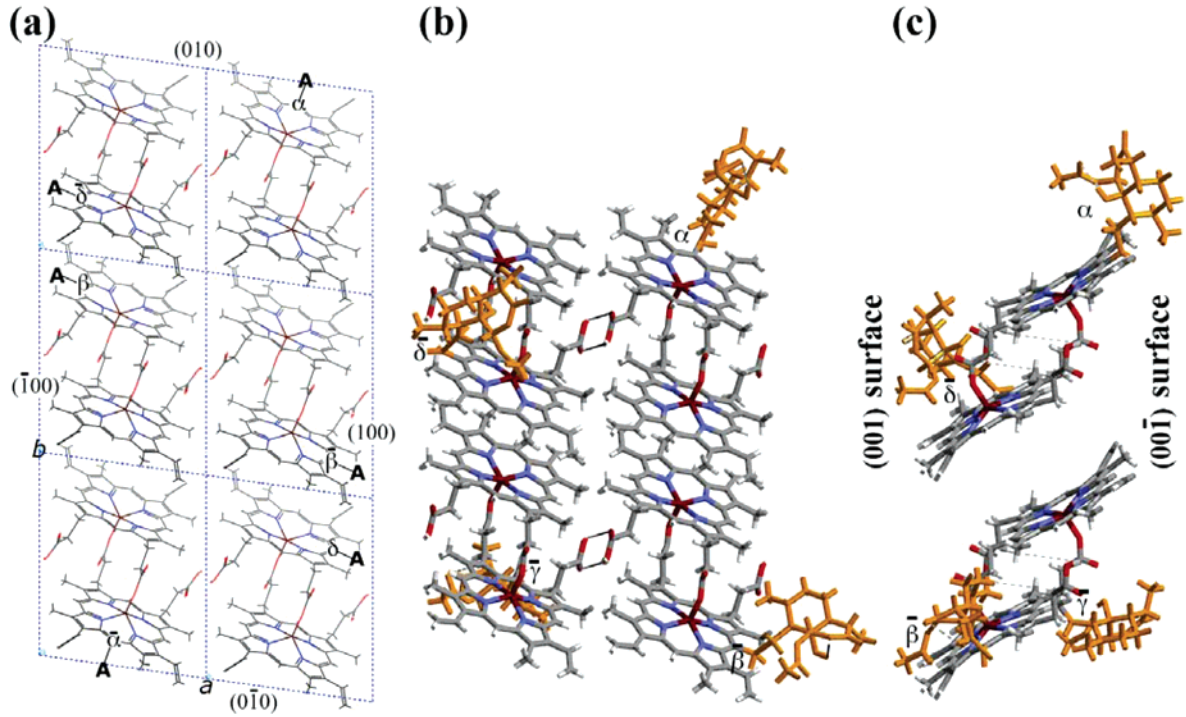

Figure 14. Arrangement of artemisinin−β-hematin dimer adducts on crystal faces of β-hematin. (a) Adsorption of the six adducts AαBH, A$\bar{\alpha}$BH, AβBH, A$\bar{\beta}$BH, AδBH and A$\bar{\delta}$BH, to the four {100} and {010} faces viewed along the *c*-axis, where A represents an artemisinin moiety covalently bound to a heme H, α, β, and δ the three peripheral sites on the heme (see Chart 2b) and BH the molecular dimer. (b, c) Views along the *c* and *a* axes of adsorption of the adducts AαBH, A$\bar{\beta}$BH, A$\bar{\delta}$BH, and A$\bar{\gamma}$BH on the various faces, where the molecular structure of the artemisinin moiety (A) bound to the hematin dimer at the different peripheral sites has been modeled by energy minimization.

not successful. Crystals do not appear to form on the water surface after spreading a fresh chloroform solution containing hemin and lutidine, or with added phospholipids DPPC or DPPE to the spreading solution, even after waiting for 24 h: one possible reason is that the hemin monomer molecules are presumably all oriented with their carboxyl groups in contact with the water surface, so that the β-hematin molecular cyclic dimer (Figure 1b) will not be formed. The solutions, when aged for about 12 h prior to being spread on the water surface, resulted in the appearance of thin oriented β-hematin crystals floating on the water surface primarily on the {100} face according to the GIXD data (Figure 3a). The average domain size of these crystals along the (100) direction was about 300 Å (Figure 3b).

The aligned parallelepiped crystals of hemozoin formed in the digestive vacuole of *Plasmodium falciparum*, displayed in the TEM image (Figure 15), reported by Goldberg and coworkers in their study on the hemoglobin degradation in *Plasmodium falciparum*[10] might yield information on the nucleation process in the digestive vacuole. These authors were struck by the fact that photographs of intact parasites show pigment crystals lined up along a single axis, whereas photographs of isolated vacuoles repeatedly show a disordered array. They suggested that the alignment may merely be an artifact of isolation or fixation or, considering the paramagnetic properties of the iron in hemozoin, that the pH gradient across the vacuolar membrane establishes an electromotive force across the vacuole that causes the pigment crystals to align within the magnetic field so generated. During isolation, the factors needed to maintain a transmembrane pH gradient may be lost, and the crystals would become disordered.

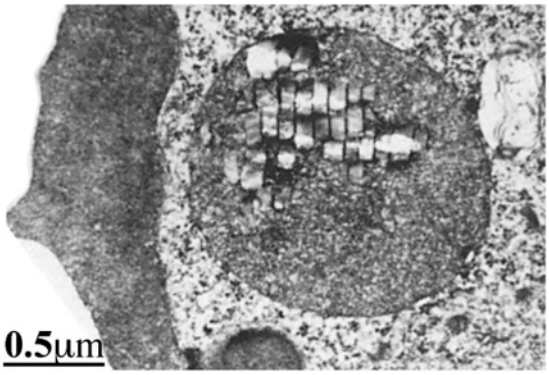

Figure 15. Electron micrograph of the digestive vacuole (dv) of a *Plasmodium falciparum* trophozoite inside an erythrocyte, showing a cluster of hemozoin crystals (bar = 0.5 μm). [Study by Goldberg et al.[10] Reproduced with permission from the author.]

We propose an alternative mechanism involving epitaxial nucleation of the hemozoin crystals via the surface of the vacuole membrane. In this respect we note that β-hematin crystallization can be promoted by lipids[1,9,39] and that neutral lipid nanospheres play a role in living parasite *Plasmodium falciparum* heme crystallization.[40] Furthermore, very recently Egan et al. reported a fast β-hematin formation under physiologically realistic conditions near octanol−water, pentanol−water, and lipid−water interfaces.[41] Given that the crystals of synthetic and biogenic hemozoin tend to grow fastest along the

(39) Bendrat, K.; Berger, B. J.; Cerami, A. *Nature* **1995**, *378*, 138.
(40) Pisciotta, J. M.; Coppens, I.; Tripathi, A. K.; Scholl, P. F.; Shuman, J.; Bajad, S.; Shulaev, V.; Sullivan, D. J. *Biochem. J.* Immediate Publication Published on October 17, 2006.
(41) Egan, T. J.; Chen, J. Y.-J.; deVilliers, K. A.; Mabotha, T. E.; Naidoo, K. J.; Ncokazia, K. K.; Langford, S. J.; McNaughton, D.; Pandiancherri, S.; Wood, B. R. *FEBS Lett* **2006**, *580*, 5105.

c-axis and are delineated by sharp {100} and {010} side faces, the crystals in Figure 15 would appear to be aligned parallel to *c*, so that the nucleation occurs via either the {100} or {010} faces. On the assumption that the nucleation is induced by exposed head groups of membranous lipids, akin to oriented nucleation of various molecular crystals via monolayers of amphiphilic molecules,[42] only a one-dimensional complementarity is required between the lipid head groups capable of forming hydrogen bonds and the propionic acid groups exposed at the {100} face of hemozoin. This model implies that the β-hematin molecular dimer would not be formed within the membrane layer, consistent with the observation (vide supra) that crystals of β-hematin were not obtained at the lipid−water interface when a fresh hemin/phospholipid chloroform solution was spread on the water surface.

The model of induced nucleation of hemozoin is also consistent with the preliminary experiments carried out in $CHCl_3$ solution on induced nucleation of β-hematin at the hydrophilic surface of a monolayer of phospholipid DBPC and hydrophobic surface of OTS; far more crystals were nucleated in the former regime. However, X-ray diffraction measurements indicated that only a very minor proportion of the β-hematin crystals were nucleated via its {100} face at the phospholipid DBPC surface, the majority of crystals were oriented randomly with respect to the {100} face.

Morphology of β-Hematin Crystals Grown in Absence and Presence of Quinolines. Information on the morphology of β-hematin crystals grown in MeOH−DMSO and $CHCl_3$ solutions were obtained from TEM measurements. The crystals were lath-like in habit. Several of these laths were symmetrically shaped, extended along the *c*-direction, and were delineated by {100} and {010} side faces and {011} end faces (Figure 6a), similar to the regular morphologies of β-hematin reported by Bohle et al.[27] Other crystals were asymmetrically tapered toward only one end of the lath (Figure 5a, d), which might be due to an irrational growth process or to the presence of a chiral impurity in the solutions used.

The pure crystals of β-hematin obtained from MeOH−DMSO solutions displayed well-developed {010} faces (Figure 6a), the {100} side face being less so, in keeping with a near rectangular crystal cross-section. The pure crystals obtained from $CHCl_3$ solution were very thin {100} laths, being almost transparent in the SEM micrographs (Figure 5e, f). We might account for this morphology as a result of binding, via an acid−base interaction, of the lutidine molecules to the exposed carboxyl group on the {100} face albeit at an oblique angle (Figure 1b), thus inhibiting growth along the *a*-direction. Here we note that the concentration of lutidine in the $CHCl_3$ solution was about 100 times greater than in the MeOH−DMSO solution.

The regular-shaped pure β-hematin crystals display the same faces {100}, {010}, and {011} as those of the theoretical growth form (Figure 2a), which is also consistent with the morphologies in some hemozoin species.[6] It is noteworthy that the side faces of several specimen crystals of hemozoin from the mammalian *Plasmodium* species, reported by Noland et al.[43] to be bricklike with smooth sides at (near) right angles, clearly correspond to the {100} and {010} side faces between which the dihedral angle is 82°. The possibility that the hemozoin side faces are of the type {110} and $\{1\bar{1}0\}$, the angle between which is 79°, may be ruled out because their crystal surfaces are highly corrugated and thus less stable than the relatively smooth {100} and {010} faces, as may be envisioned from Figure 1b, in agreement with theoretical growth form computations.[6]

Model of Quinoline Binding to the Crystal Faces of β-Hematin. Regarding experimental evidence establishing the direction of the inhibition of growth of hemozoin crystals via the proposed surface binding site of quinoline-type drugs to the {001} face, we had suggested[6] that the darker areas at the {001} end faces terminating the longer sides of several aligned hemozoin crystals, reported by Goldberg and co-workers,[4] correspond to adsorbed or occluded [H^3]chloroquine. However, Egan, in a comprehensive review on hemozoin as a unique crystalline drug target,[44] remarked that the dark areas may merely be regions of increased electron density, although it would be unusual that tabular shaped crystals are thicker at its ends. The doubts raised by Egan, however, imply the need for unambiguous evidence in favor of the crystal surface-binding model. We found that β-hematin crystals grown from MeOH−DMSO and $CHCl_3$ solutions in the presence of quinoline additives display, in a significant amount, crystals tapered at both ends, which are highly symmetric in shape (Figures 5b, c, e, f and 7a). We propose that such tapering is adopted in order to help reduce inhibition of growth along the *c*-axis by adsorption of the quinoline additive on the {001} or {011} faces expressed as ledges in the proposed stepped-face morphology shown in Figure 7b, resulting in a spine formation of thinner and thinner cross-section. It is of relevance that crystals of *R,S*-alanine and of ammonium dihydrogen phosphate are also symmetrically tapered when respectively grown in the presence of additive *S*-threonine[45] and particular ionic species[46], a possible explanation being that in this way the inhibiting effect is somewhat ameliorated. In order to provide supporting evidence to the model of quinoline adsorption and crystal growth inhibition, the effect of quinine on *R,S*-mandelic acid crystallization was examined (see SI). We found that quinine inhibits the nucleation and growth of *R,S*-mandelic acid, explained by acid−base binding of the additive to the crystal faces exposing carboxyl groups.

Analysis of the synchrotron powder X-ray diffraction data of pure and affected β-hematin, grown in the absence and the presence of quinine and chloroquine respectively, suggests, for the crystals grown in chloroform solution, that the additives reduce the crystal mosaic domain size along the *c*-direction (see Table 1). The coherent grazing X-ray diffraction data of pure and affected β-hematin, the latter obtained from MeOH−DMSO solution, appear to be consistent with the above conclusion.

Examination of the Raman spectra in Figure 10 and the infrared spectra in Figure 12 shows no direct evidence of the presence of quinine or chloroquine in any spectra but does show that there are minor, but distinct, changes between quinoline-affected and pure β-hematin crystals. The observed differences in both PCA scores plots (Figure 11a,b) may be explained in terms of the effect of stereoselectively bound quinoline occluded within the bulk of the crystal: the centrosymmetric β-hematin

(42) Weissbuch, I.; Lahav, M.; Leiserowitz, L. *Cryst. Growth Des.* **2003**, *3*, 125−150.
(43) Noland, G. S.; Briones, N.; Sullivan, D. J. *Mol. Biochem. Parasitol.* **2003**, *130*, 91−99.
(44) Egan, T. J. *Targets* **2003**, *2*, 115−124.
(45) Weissbuch, I.; Leiserowitz, L.; Lahav, M. *Adv. Mat.* **1994**, 953−956.
(46) Davey, R. J.; Mullin, J. W. *J. Cryst. Growth* **1974**, 89.

molecular dimers in the vicinity of such poisoned sites, which are asymmetric imparting a local symmetry reduction, undoubtedly adjust their positions to fit into the regular crystal arrangement.

The loadings plots for the Raman data show that both antimalarials have chemically changed the β-hematin and that the changes are commensurate with changes in bands sensitive to lattice perturbation. The enhancement of bands in aggregated heme systems is thought to involve excitonic interactions, where energy in the form of an exciton can migrate throughout the extended porphyrin network due to overlap of π-orbitals[11] This leads to the increase in amplitude of predominately totally symmetric modes such as ν_2 and ν_4 at 1566 and 1377 cm^{-1} but also some B_{1g} modes at 1551 cm^{-1} (ν_{11}) and 1626 cm^{-1} (ν_{10}). The reduction in intensity of these bands in the quinoline-affected samples is attributed to a perturbation in the porphyrin aggregate that impedes exciton migration in the aggregate, resulting in the decrease in amplitude of A_{1g} and B_{1g} modes.

The infrared spectral variations between the three samples show changes in the major involved in the propionate linkages (vide supra). For the cluster map (Figure 12) of the combined data set there is a distinct separation between pure β-hematin and both quinoline-affected β-hematin samples choosing either 2, 3, 4, or 5 clusters, showing that there is great spectral similarity between crystals grown in the presence of the quinoline additives. Apart from changes in bands due to propionate linkages, the small band at 1744 cm^{-1}, observed in the second derivative spectra and attributed to surface propionic acid groups in β-hematin, is essentially absent in the quinoline-affected samples. These changes indicate that the quinoline have indeed modified the crystal surface by binding to the surface acid groups. The Raman data on the other hand indicate the quinoline has perturbed the β-hematin lattice.

All in all, there seems to be little doubt as to the model of quinoline binding to the {001} and {011}, as well as, perhaps, the {100} faces of hemozoin,[6] leading to inhibition of crystal nucleation and growth. During this process a quinoline molecule may also bind to a β-hematin molecular dimer before the latter is adsorbed on a crystal surface, as proposed by Sullivan and Chong,[29] but which has a kinetic disadvantage that the complex must "locate" the appropriate face, (001) or $(00\bar{1})$, onto which to adsorb, depending upon to which of the two carboxyl groups the drug is bound. Naturally if both carboxyl groups of a β-hematin molecular dimer are bound to quinoline, such a complex cannot be stereoselectively adsorbed onto the crystal surface and so will be ineffective as an inhibitor.

Possible Mechanisms of Antimalarial Action of Diethylamino-alkoxyxanthone and Artemisinin-Type Drugs. The antimalarial activity of the diethylamino-alkoxyxanthone drugs had been explained by Riscoe and co-workers[13,14] in terms of the binding constant of the drug to heme in solution (see SI, Figure S1). We propose hemozoin as a primary drug target, involving binding of the drug to the {001}, {011}, and perhaps {100}, crystal faces, leading to inhibition of crystallization. The computed binding energy of the drug to the crystal faces is dependent upon the drug chain length (Table 2). Comparing the antimalarial activity of drugs XN2 and XN5, the latter, with chain lengths appropriate for the two terminal amino groups to bind simultaneously to two carboxyl groups exposed at the {001} or {011} faces and also form favorable van der Waals contacts with the crystal face (Figure 13), is a better antimalarial. This crystal surface binding model also accounts for the reduced antimalarial activity for molecules XN8 (SI, Figure S1) being about 6 Å longer than XN5 and so would bind to the two surface carboxyl groups on the {001} or {011} faces only if the molecular chain would be bent and thus make poorer van der Waals contact with the crystal surface. The efficient antimalarial potency of diamidines, another class of novel drugs embodying proton donor groups (amidine) at either end of the molecule, has been reported some years ago.[47] These authors showed that diamidines inhibit hemozoin formation in vitro with a similar potency to chloroquine. It is likely that these drugs, such as pentamidine ($H_3N_2C-C_6H_4-O-C_5H_{10}-O-C_6H_4-CN_2H_3$) inhibit hemozoin formation as a result of binding of both amidine groups of the molecule to exposed propionic acid groups at the crystal surface. Of relevance to the model proposed for antimalarial action of the diethylamino-alkoxyxanthones is growth inhibition of barium sulfate by an additive with moieties which simultaneously cap onto the crystal surface.[48] Another example, (described in SI), is the crystal nucleation retardation of *S*-alanine by different diamine derivatives, the most effective being an additive with a central chain, the length of which matches the distance between two carboxylate groups exposed at the crystal surface.

Regarding antimalarial action of artemisinin-type drugs, we have described a model involving reaction of four artemisinin−heme-type adducts, (Chart 2b), with a free heme monomer to yield eight derivatives of the cyclic β-hematin dimer, comprising four diasteroisomeric pairs which may bind to the {100}, {010}, and {001} faces of a β-hematin crystal shown in Figure 14. Such molecules, if present in the digestive vacuole of the parasite, would act in a manner akin to that of a classic tailor-made additive in solution designed to inhibit crystal nucleation and growth.[42] According to this model, crystal growth of hemozoin may be inhibited along all three principal crystal directions, *a, b*, and *c*, consistent with the report that artemisinin inhibits hemoglobin digestion by malaria parasites and inhibits hemozoin formation,[17] but which has only been demonstrated in cell-free conditions. We stress, in terms of the model presented here, that efficient inhibition of hemozoin formation via artemisinin would seem possible, provided the cyclic β-hematin dimer derivatives are formed in the digestive vacuole of the parasite; the artemisinin−heme-type adducts (Chart 2b) would not be as strongly adsorbed on hemozoin crystal surfaces to act as efficient growth inhibitors.

According to the model only a small fraction of the ensemble of artemisinin−cyclic β-hematin dimer adducts can be adsorbed onto the small, but fast-growing {001} faces. We may therefore rationalize why artemisinin-based combination therapy (ACT) involving artemisinin and quinoline drugs is more effective than each of them applied separately in clinical studies combating malaria.[49−51] The improved efficacy might be explained as

(47) Stead, A. M. W.; Bray, P. G.; Edwards, I. G.; Dekoning, H. P.; Elford, B. C.; Stocks, P. A.; Ward, S. A. *Mol. Pharmacol.* **2001**, 1298.
(48) Coveney, P. V.; Davey, R.; Griffin, J. L. W.; He, Y.; Hamlin, J. D.; Stackhouse, S.; Whiting, A. *J. Am. Chem. Soc.* **2000**, *122*, 11557.
(49) deVries, P. J.; Bich, N. N.; Thien, H. V.; Hung, L. N.; Anh, T. K.; Kager, P. A.; Heisterkamp, S. H. *Antimicrob. Agents Chemother.* **2000**, *44*, 1302−1308.
(50) Gupta, S.; Thapar, M. M.; Mariga, S. T.; Wernsdorfer, W. H.; Bjorkman, A. *Exp. Parasitol.* **2002**, *100*, 28−35.
(51) Olliaro, P. L.; Taylor, T. W. *J. Postgrad. Med.* **2004**, *50*, 40−44.
(52) Wei, K.-T.; Ward, D. L. *Acta Crystallogr.* **1977**, *B33*, 797−800.

follows: quinoline drugs are expected to inhibit growth primarily along the fast-growing needle *c*-axis, and the artemisinin-type drugs have been hypothesized to retard growth along all three principal crystal directions (*a*, *b*, *c*). Thus, a combination of these two types of drugs would be effective inhibitors of overall crystal formation of hemozoin because of a relatively high concentration of drugs available for binding onto the small, yet fast-growing, opposite faces terminating the needle. This hypothesis is in agreement with the experiments on the model crystal system *S*-alanine, suggesting that a combination of tailor-made additives that bind to different crystal surfaces has a greater inhibiting effect on nucleation than each of the additives used alone.

Concluding Remarks

The most dominant crystal faces of β-hematin have been experimentally characterized, in agreement with the shape of some reported hemozoin crystals and the theoretical growth form of β-hematin.[6] An effect of quinine and chloroquine on the growth morphology of β-hematin has been observed and correlated with adsorption of the drugs onto the {001} or {011} crystal faces. This interpretation is in agreement with evidence, although marginal, from synchrotron X-ray diffraction data of powder samples that the quinoline additives reduce the crystal domain size along the *c*-axis and with coherent grazing X-ray diffraction experiments, which suggest that the β-hematin crystals grown in the presence of the additives were smaller and less structurally stable than the pure form. The IR-ATR and Raman spectral results show that β-hematin grown in the presence of the quinoline drugs embodies molecular based differences from pure β-hematin. The results suggest modification of surface and bulk propionic acid linkages and aggregation perturbation within the affected crystal, albeit minor, presumably arising from host molecular rearrangement in the environment of the bulk sites poisoned by occluded quinoline. These proposed changes are consistent with the interpretation of morphological modification, the X-ray diffraction results, and the model computations of surface binding of quinoline antimalarials to the {001} face of β-hematin.[6]

Computational studies carried out on the antimalarial diethylamino-alkoxyxanthanones suggest that the hemozoin crystal is a primary drug target, via stereoselective binding of the two amine groups of the molecule to acid groups exposed at the crystal surface, resulting in inhibition of hemozoin nucleation or growth. A model is proposed for the antimalarial action of artemisinin-type drugs involving efficient inhibition of crystal nucleation of hemozoin by binding onto all principal crystal faces, thus acting akin to classic tailor-made inhibitors of crystal nucleation. This model might also explain the effective antimalarial properties of a combination of artemisinin-type drugs and quinolines, assuming that the latter will inhibit growth along the fast-growing but small faces at the opposite ends of the needle-shaped hemozoin crystal.

A model has been presented of induced epitaxial nucleation of hemozoin via a lipid membrane in the digestive vacuole of a malaria parasite, based on a published electron micrograph of the digestive vacuole of a *Plasmodium falciparum* trophozoite inside a red blood cell, showing a cluster of aligned hemozoin crystals (Figure 15).[10] Studies on oriented nucleation of β-hematin crystals at the interface between lipid monolayers and water, or other liquids, are currently being undertaken.

Acknowledgment. This work was supported in part by the Kimmelmann Center at the Weizmann Institute of Science, the DanSync program of the Danish Natural Science Research Council, the Carlsberg Foundation and the European Community under TMR-Contract ERBFMGECT950059. Thanks are due to HASYLAB for synchrotron beamtime and to Professor Jochen Schneider, Director of HASYLAB. Regarding use of beamtime at the Advanced Photon Source, the UNICAT facility is supported by the Materials Research Laboratory, University of Illinois funded by U.S. DOE award DEFG02-91ER45439, the Oak Ridge National Laboratory, the National Institute of Standards and Technology and UOP LLC. Part of this work is funded by an Australian Research Council Discovery Grant. B.R.W.'s work is supported by an Australian Synchrotron Program Fellowship Grant and a Monash University Synchrotron Fellowship Grant.

Supporting Information Available: Experimental Section; Figure S1 showing the reported[13] effect of carbon chain length on the antimalarial activity (IC_{50}) and heme affinity (K_a) of diethylamino-hydroxyxanthone molecules; section describing inhibition of crystal nucleation of *R,S*-mandelic acid with quinine; section describing a computational study on binding of diethylamino-alkoxyxanthones to β-hematin crystal faces in correlation with antimalarial activity; section describing a model study on inhibition of crystal nucleation of *S*-alanine via additive combinations. This material is available free of charge via the Internet at http://pubs.acs.org.

JA0674183